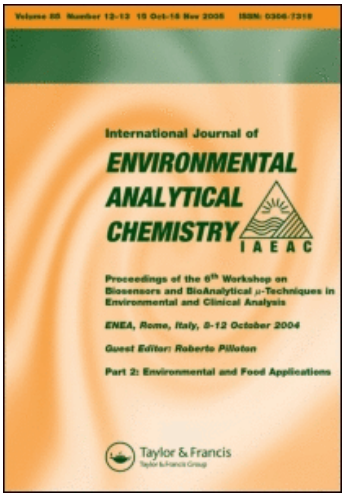

International Journal of Environmental Analytical Chemistry
Publication details, including instructions for authors and subscription information:
http://www.informaworld.com/smpp/title~content=t713640455

Quantitative Assessment of a Corona Discharge Ion Source in Atmospheric Pressure Ionization-Mass Spectrometry for Ambient Air Monitoring

G. A. Eiceman[ab]; J. H. Kremer[cd]; A. P. Snyder[c]; J. K. Tofferi[c]
[a] Department of Chemistry, New Mexico State University, Las Cruces, NM, USA [b] US Army Chemical Research, Development, and Engineering Center, MD, USA [c] US Army Chemical Research, Development and Engineering Center SMCCR-RSL, MD, USA [d] Wehrwissenschaftliche Dienststelle der Bundeswehr fũer ABC-Schutz, Humboldtstrasse, Munster, FRG

To cite this Article Eiceman, G. A. , Kremer, J. H. , Snyder, A. P. and Tofferi, J. K.(1988) 'Quantitative Assessment of a Corona Discharge Ion Source in Atmospheric Pressure Ionization-Mass Spectrometry for Ambient Air Monitoring', International Journal of Environmental Analytical Chemistry, 33: 3, 161 — 183
To link to this Article: DOI: 10.1080/03067318808081669
URL: http://dx.doi.org/10.1080/03067318808081669

Intern. J. Environ. Anal. Chem., Vol. 33, pp. 161–183
Reprints available directly from the publisher
Photocopying permitted by license only

Printed in Great Britain

Quantitative Assessment of a Corona Discharge Ion Source in Atmospheric Pressure Ionization-Mass Spectrometry for Ambient Air Monitoring

G. A. EICEMAN*

Department of Chemistry, New Mexico State University, Las Cruces, NM 88003-0003, USA

and

J. H. KREMER,† A. P. SNYDER and J. K. TOFFERI

US Army Chemical Research, Development and Engineering Center SMCCR-RSL, Aberdeen Proving Ground, MD 21010-5423, USA

(*Received 22 July 1987; in final form 3 November 1987*)

In a corona discharge (CD) source for atmospheric pressure ionization-mass spectrometry (API-MS), ion abundances and signal stability for reactant ions in ambient air were governed by gap size, discharge current, and point-to-plane alignment. Reactant ion currents were related directly to discharge current fluctuations and varied 3–20% RSD with a 5 mm gap where ion intensities were greatest. Relative abundances for reactant ions were insensitive to source parameters with 10–30 mm gaps, however, absolute ion intensities were decreased more than 90%. Product ions were formed from gaseous analyte in air through collisional proton-transfer from reactant ions and intensity and variance for product ions paralleled

*Present address: US Army Chemical Research, Development, and Engineering Center, SMCCR-RSL, Aberdeen Proving Ground, MD 21010-5423, USA.

†Present address: Wehrwissenschaftliche Dienststelle der Bundeswehr fuer ABC-Schutz, Humboldtstrasse, D3042 Munster, FRG.

reactant ion trends. Product ion spectra were complicated by masses 91–163 amu from higher hydrated reactant ions with high intensity in the CD source. Response curves for product ions agreed with existing low-field API rate theory and competitive ionizations with analyte mixtures showed selective distribution of available protons. Preferential depletion of reactant ions by product neutrals was not observed and user-directed selectivity through control of ionization with reactant ions naturally abundant in ambient air alone seemed unpromising.

KEY WORDS: Ionization-mass spectrometry, absolute ion, ion intensities.

INTRODUCTION

Atmospheric pressure ionization-mass spectrometry (API-MS) was described originally in 1973 and used for rapid detection of drugs in unpurified biological extracts.[1,2] In API-MS measurements, analyte is ionized collisionally through proton- or electron-transfer with reactant ions. The nature and properties of such mechanisms are responsible for picogram detection limits and extraordinary specificity for samples of complex chemical composition. Thus, development of API-MS in analytical chemistry was motivated by simplicity of sample preparation and speed of analysis. While β-particles from ^{63}Ni were used in early API-MS for generation of reactant ions, corona discharge (CD) was viewed as an alternate ion source based on studies with inorganic gases at 0.4–1 torr.[3–6] In CD sources, hydrated-proton cluster ions with a formula $(H_2O)_nH^+$, where $n=$ 2–9, are created through release of electrons from an electrically stressed metal electrode into ambient air or supporting gases. These hydrated-proton cluster ions can then be used as a reservoir of charge (e.g. reactant ions) for gentle ionization of gaseous analyte (M) principally to MH^+.

While stable CD currents have been sustained with wire-coaxial tube designs, a more common geometry in analytical API-MS has been a point-to-plane geometry. Pulseless current discharges of 1–10 μA are established between part of the mass spectrometer (MS) flange at low potential and a metal needle at 3–6 kV. Corona discharges were considered attractive initially since ionization processes might be controlled through contact times between analyte and reactant ions.[7] Furthermore, signal intensities were strong compared to other API sources perhaps since ion depletion through recombination reactions may be relatively small. Corona discharge has not become a common ion source in MS and allied ion

separation techniques but instead has acquired a general reputation for instability and poor reproducibility. Although corona phenomena have been studied since the 1930s[8] and used in MS since the mid-1960s,[3,4] source effects on actual atmospheric monitoring have not been described. For example, current-voltage-distance properties in a CD are known,[9] but the consequences for stability, selectivity, and sensitivity in API-MS measurements are unclear. Thus, a present concern is the potential use and acceptance of API-MS and API-MS/MS equipped with CD sources for ambient air monitoring[10,11] while source influences in ion formation and subsequent MS measurements are undefined.

Ion formation in a CD has been studied as a function of point-to-plane distances and gas compositions[3–6] but only for low vacuum conditions with nitrogen gas. Highly complex chemistry with the ion-molecule reactions was suggested from these studies. Nonetheless, an elementary theory proposed for API reactions in electric fields has been validated[13] and might be suitable for application to a CD source in ambient air. This investigation represents the first reported quantitative assessment of CD properties for air monitoring by API-MS. Such a description will contribute to the evaluation of CD for quantitative MS measurements, selection of CD parameters for optimum analytical response, and improvement of existing CD designs. A detailed description of effects from CD parameters will also facilitate incorporation of this source into other inexpensive API-based air sensing devices such as ion mobility spectrometers.[14] A final objective was an exploration of user-control of analyte ionization in a CD according to early claims in API-MS literature.

EXPERIMENTAL

Instrumental

The mass spectrometer was a Sciex, Inc. (Toronto, Ontario, Canada) TAGA 6000MS/MS equipped with a Digital Equip. Corp. PDP 11/23 minicomputer, Tektronix Model 4025 terminal, and Tektronix 4631 hard copy unit. The CD source shown in Figure 1 was kept at atmospheric pressure and was separated from the MS vacuum by a conductive foil membrane with a 40 μm diameter pinhole. The CD was a current-regulated point-to-plane design with

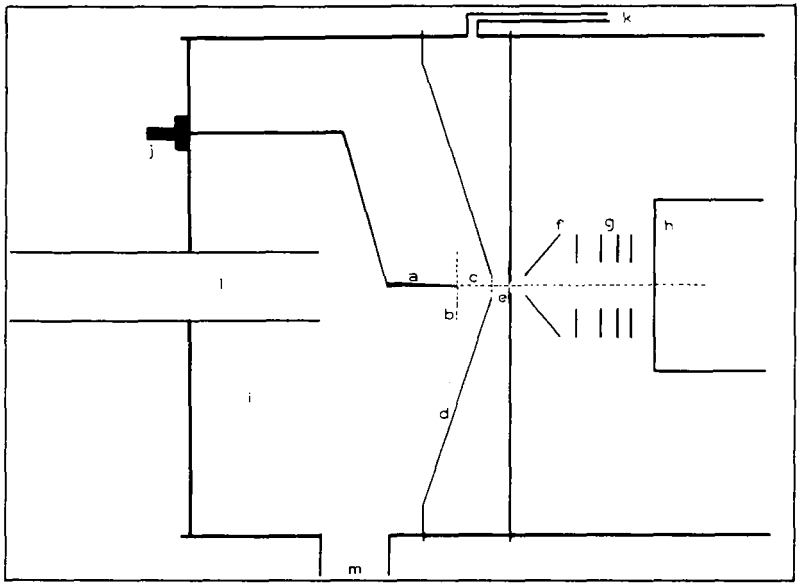

Figure 1 Schematic of the corona discharge ion source in API-MS for ambient air monitoring. The geometry of this source resembles most a point-to-plane design even though the plane has a slight conical shape. Labelled components or parameters are: (*a*) darning needle used for discharge, (*b*) axial displacement of needle from orifice center, (*c*) vertical displacement of needle from discharge plate (or plane), (*d*) plate used to establish discharge with needle, (*e*) pinhole foil where ions pass from atmospheric pressure to vacuum, (*f*) declustering lens, (*g*) lens assembly, (*h*) quadrupole mass spectrometer, (*i*) API source volume, (*j*) micrometer control for needle position, (*k*) curtain gas inlet, (*l*) sample gas (ambient air) inlet, and (*m*) suction pump for sample gas.

large physical dimensions that afforded low memory effects. The point electrode was a common darning needle and the plane was part of the MS vacuum flange, though slightly conical in shape. A flow of dry nitrogen called the curtain gas was used to sweep the pinhole free of any particulate matter. Sample gas (unpurified ambient air) was drawn into the source using an electric suction pump and confluence with the curtain gas occurred in the discharge region. All instrumental conditions are listed in Table 1; changes are cited as needed in figure captions and in procedures described below. The MS was operated using both scanning and selected ion moni-

Table 1 Instrumental parameters for API-MS operation with a corona discharge ion source

Parameter	*Range of experimental values; nominal values*
Source:	
Discharge current	0.1 to 10 μA; 3 μA
Flow rate for sample gas	20 to 100 L/min; 25 L/min
Plane potential	650 V
Curtain gas flow rate	10 to 1000 mL/min; 230 mL/min
Lens:	
Lens 1	63 V
Declustering lens, lens 2	43 to 63 V; 48 V
Lens 3	39 V
Scanning MS:	
Initial mass	50 amu
Final mass	200 amu
Scan rate	10 amu/ms
No. scans per spectrum	28
Delay between scans	0.5 ms
Electron multiplier voltage	3650 V
Threshold value[a]	1000
SIM MS:	
Ion masses: Reactant ions	m/z 37, 55, 73 and 91
Ethylacetate	m/z 89, MH^+; 107, $M(H_2O)H^+$
Triethylamine	m/z 102, MH^+
DMMP	m/z 125, MH^+
Dwell times	200 ms

[a]Abundances less than 1000 counts were rejected as unreliable.

toring (SIM) modes while the second and third quadrupoles were operated in the RF mode and were functionally transparent. All instrumental conditions except gap size and gas flows were controlled from the minicomputer. A Nupro fine metering valve (Willoughby, OH) was added for control of the curtain gas flow and the gap size was set manually using a micrometer. A Simpson digital multimeter Model 463 was connected to the discharge supply control board so CD voltages could be measured directly.

Procedures

Reactant ion studies. Influences from electrical, physical, and flow

parameters in a CD source on MS response were measured using four separate studies. In each study, one or two parameters were varied between operating extremes and 5–10 measurements were collected per parameter. For a current/voltage/distance study, gap sizes were set between 1–30 mm and discharge currents were set from 0.1–10 μA. The influence of axial position of the needle was measured with axial offsets of 0–60 mm from the orifice center and at two gap sizes of 5 and 10 mm. Effects of mixing curtain gas and sample gas were evaluated with curtain gas flows of 95–400 mL/min and sample gas flows of 20–100 L/min with 5 mm and 10 mm gaps and 3 μA discharge current. The role of a declustering lens (lens 2) voltage was evaluated with a 5 mm gap and lens voltages from 41 to 63 V which corresponded to a potential drop of 0 to 22 V between the declustering lens and the source plane.

Product ion studies. Three studies were made to evaluate the effects of CD parameters on API-MS response to analyte in ambient air. Response curves were obtained for three compounds, ethylacetate (EtOAc), triethylamine (TEA), and dimethylmethylphosphonate (DMMP) by metering vapors from headspace over pure liquids into the sample gas at 50 L/min. Analyte concentrations in the source were calculated using known vapor pressures and dilution ratios. In a second part, small amounts of one analyte were metered into the sample gas at a fixed rate while a response curve was generated with a second compound. In a final study, known fixed amounts of single analyte were added into the sample gas while source parameters including gap size, discharge current and curtain gas flow were individually varied; product ion intensities were measured continuously using SIM methods.

RESULTS AND DISCUSSION

Reactant ions in ambient air

In Figure 2, the region of sustained or continuous discharge in ambient air is shown for a CD source in API-MS. When source parameters not defined by the curves in Figure 2 were used, discharge currents became highly erratic. Previously, three regions of

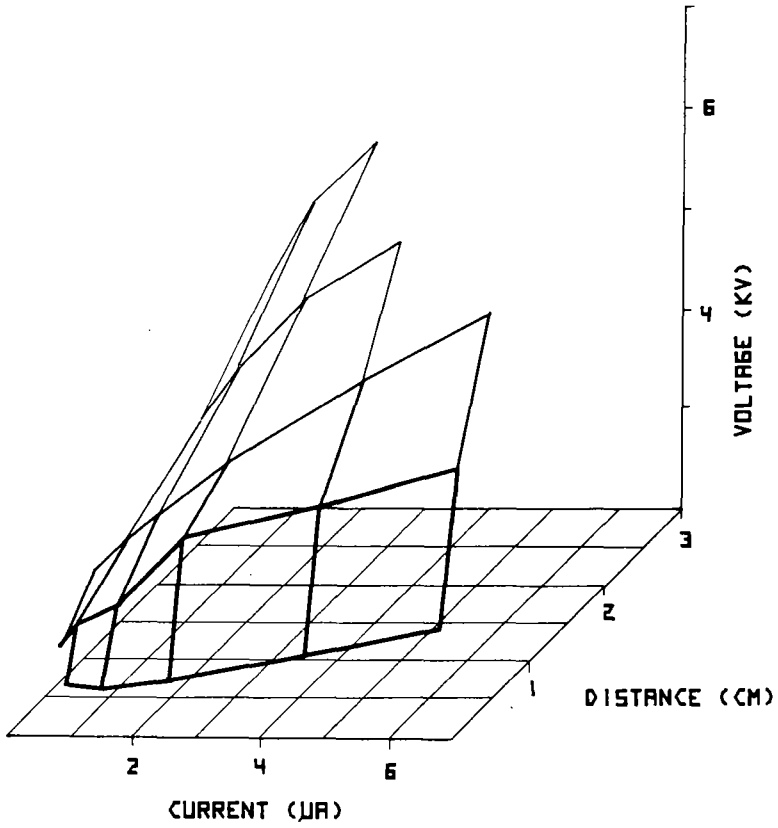

Figure 2 Plot of currents, voltages, and gap distances for a pulseless corona discharge in ambient air at atmospheric pressure. At fringes of the plot, the discharge became highly erratic or exhibited breakdown behavior.

CD behavior had been identified and included (*a*) pre-onset streamers below the threshold voltage, (*b*) pulseless glow corona with currents of 1–15 μA, and (*c*) periodic breakdown streamers with fields >15 kV/cm.[9] Thus, stable CD performance here was bracketed by unstable behavior on extremes by pre-onset streamers at low voltages and by breakdown streamers at high voltages. Although the region of pulseless discharge in air extended from 3.1–6.6 kV, 2.5–30 mm, and 0.20–6.60 μA, fluctuations in total abundances for reac-

tant ion spectra were observed throughout the operating region. The influence of source parameters on such fluctuations is shown partially in Figure 3. While reproducibility of normalized ion abundances was good between 1–6 μA, use of parameters at or near operating CD extremes $<1\,\mu$A or $>6\,\mu$A (or <5 mm and >30 mm) was reflected directly as increased fluctuations in total ion abundances. Comparison of standard deviations for currents listed in Table 2 showed that comparable trends occurred for all gap sizes. Thus, discharge currents measured directly on the CD and ion currents in mass spectra for reactant ions in air were both indicative of corona instability from either pre-onset or breakdown streamers.

Absolute intensities for reactant ions were also affected by the gap size and discharge currents as shown in Table 3. For example, a 59-fold increase in abundance for m/z 55 was seen between 0.5–7.5 μA while the absolute standard deviation increased only 2.9-fold. Comparable trends were observed with other gap sizes. These findings can be used to predict the number of scans needed to acquire a representative mass spectrum. The number of scans needed to yield 99.7% probability that ion abundances for a 5 mm gap will be within one standard deviation at each discharge current were: 324, 0.5 μA; 1, 1 μA; 14, 6 μA; and 37, 7.5 μA. Although appropriate adjustments of source parameters can reduce acquisition times for a representative spectrum from over 3 minutes to only 15 s, more than 100 scans will not necessarily ensure good precision if source parameters are chosen poorly. Atmospheric resistivity in the discharge region was dependent upon the electric field as is consistent with Chapman's report that CD currents were proportional to both voltage and ion velocity.[15] Field-dependent ion velocities according to the Nernst–Einstein formula[16] were supported by E/N calculations and ambient air exhibited distinctly non-Ohmic behavior with a CD source in air.

Hydration-numbers for reactant ions in air

Effects of current and distance on relative abundances of reactant ions in API-MS are shown in Table 4 and in Figure 4 where the influence of source parameters on hydration numbers for reactant

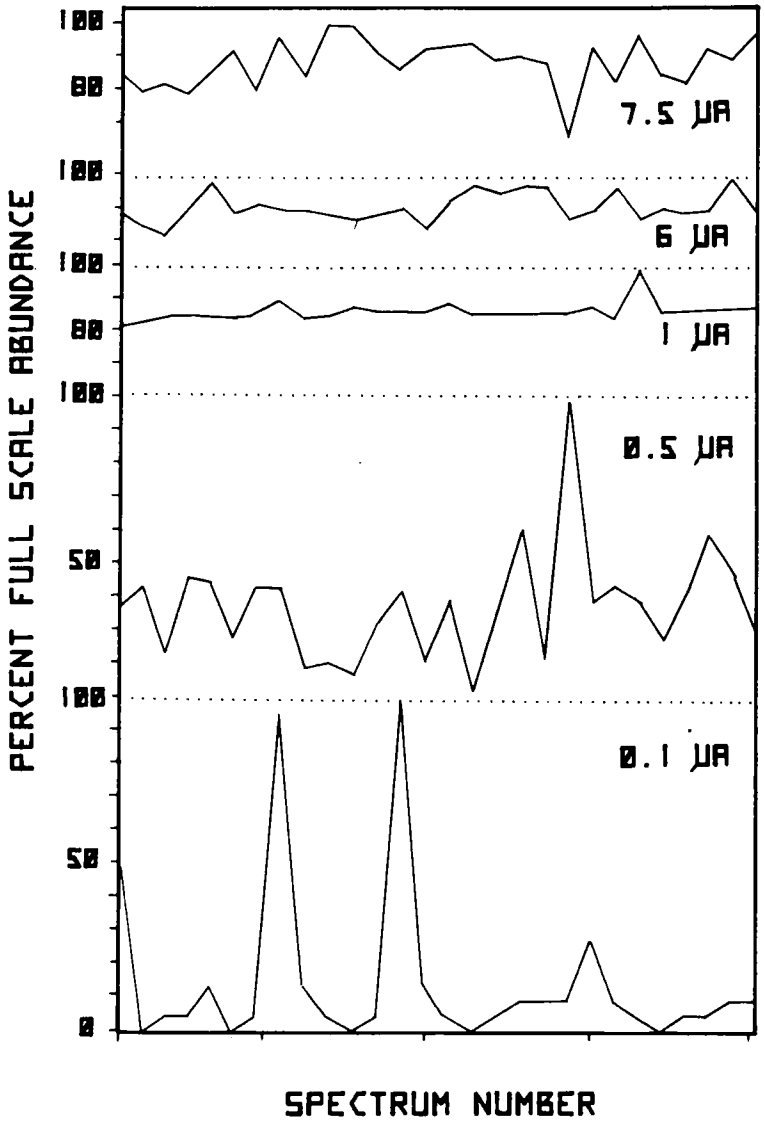

Figure 3 Total abundances for naturally abundant reactant ions in ambient air from replicate mass spectra. Full scale values for total ion abundances($\times 1\,000\,000$) at each discharge current setting were 7.4 μA, 6.11; 6 μA, 5.69; 1 μA, 3.58; 0.5 μA, 3.99; and 0.1 μA, 0.02. Gap size was 10 mm. Tabular data from spectra are given in Table 3.

Table 2 Physical and electrical properties of a corona discharge in ambient air for API-MS

Gap size (mm)	*Parameter*[b,c]	*Nominal discharge current, μA*[a]					
		0.1	*0.5*	*1*	*2*	*4*	*6*
2.5	V (kV)	3.1	3.1	3.2	3.3	3.6	3.9
	I (μA)	0.82	0.63	1.90	2.40	4.40	6.50
	SD	0.02	0.66	2.7	0.26	0.12	0.12
	% RSD	18	100	140	11	2.6	1.9
5.0	V	3.5	3.7	3.9	4.3	4.8	5.3
	I	0.19	0.64	1.20	2.30	4.40	6.50
	SD	0.05	0.02	0.02	0.02	0.02	0.05
	%RSD	25	2.5	1.5	0.80	0.5	0.7
10	V	3.9	4.1	4.4	4.9	5.8	6.5
	I	0.20	0.65	1.20	2.30	4.40	6.60
	SD	0.03	0.02	0.02	0.04	0.04	0.03
	%RSD	15	2.8	2.1	1.5	0.48	0.50
20	V	4.2	4.6	5.1	5.9	6.6	**[d]
	I	0.21	0.64	1.20	2.03	3.70	**
	SD	0.02	0.02	0.02	0.02	0.08	**
	%RSD	10	2.8	1.5	0.95	2.1	**
30	V	4.6	5.3	6.0	6.6	**	**
	I	0.22	0.65	1.22	1.82	**	**
	SD	0.09	0.02	0.16	0.07	**	**
	%RSD	39	3.4	13	4.0	**	**

[a]The nominal discharge current was set via the PDP 11/23. The keyboard selected current and actual currents typically differed by from 0.1 to 0.5 μA.

[b]Voltages were normally stable to better than ±0.01 kV. When unstable, voltages followed a sawtooth waveform and mean values were estimated.

[c]Each current value was averaged from 15 replicate measurements.

[d]** indicates complete instability in the CD source.

ions is illustrated. As shown in Table 4, increases in discharge current or decreases in gap distance caused increases in relative abundance of ions with large *n* values. Generally, CD gaps >5 mm were insensitive to current effects on *n* while relative abundances for gaps <5 mm were influenced dramatically by currents. Thus, spectral insensitivity to source parameters occurred near 10 mm between 1 to 6 μA and coincided with the region of greatest stability electrically and chemically in the CD. However, greatest absolute reactant ion

Table 3 Intensities for reactant ions in ambient air at atmospheric pressure from a corona discharge

Nominal current (μA)	*Parameter*	*Ion mass (amu)*			
		37	*55*	*73*	*91*
0.1	Intensity[a]	**[b]	**	**	**
0.5	Intensity	70 000	26 000	2 000	**
	SD	44 000	29 000	2 000	**
	%RSD	6.3	110	100	**
1.0	Intensity	1 306 000	686 000	62 000	5 000
	SD	32 000	84 000	9 000	1 000
	%RSD	2.5	12	14	20
6.0	Intensity	1 504 000	1 437 000	475 000	56 000
	SD	192 000	97 000	175 000	52 000
	%RSD	13	6.8	37	93
7.5	Intensity	1 422 000	1 536 000	590 000	85 000
	SD	288 000	85 000	225 000	59 000
	%RSD	20	5.5	38	69

[a]Intensity was abundance units (counts/s) averaged from 28 replicate spectra.
[b]Spectra at 0.1 μA contained no ions except for spectra that coincided with pre-onset streamers.

abundance was found at 5 mm and 2–4 μA as shown in Figure 5 and in this region MS response was seriously affected by source parameters. Causes for such differences may be due to (*a*) changes in efficiency (kinetics) of formation of individual ions, (*b*) changes in cluster-ion survival (declustering) from creation to injection into the MS, or (*c*) other unidentified processes. Since the declustering lens potential was kept constant through these studies, observations here reflect actual changes in CD chemistry rather than in sampling artifacts with the MS. While causes have not been determined, the analytical consequences in atmospheric sensing of contaminants using API-MS may include effects on sensitivity, selectivity, and reproducibility. For example, the CD is likely not in thermodynamic equilibrium and since proton affinities of these cluster ions may differ by >5 kcal/mole, control kinetically of chemical selectivity or sensitivity through adjustment of principal reactant ions was an interesting though unproven possibility.

Table 4 Tabular mass spectra for reactant ions in ambient air from corona discharge API-MS. The principle reactant ions were $(H_2O)_nH^+$ ions where $n=2$ to 9. The declustering lens was fixed at 48 V

Gap size (mm)	*I (μA)*	*Percent relative abundance*[a]							
		Ion masses (amu) (n)							
		37 *2*	*55* *3*	*73* *4*	*91* *5*	*109* *6*	*127* *7*	*145* *8*	*163* *9*
2.5	0.1	12.5	6.8	100.0	85.2	20.5	0	0	0
	0.5	100.0	89.0	74.9	62.7	11.4	6.1	13.1	6.7
	1.0	48.9	76.0	100.0	56.9	29.2	16.3	14.1	6.6
	2.0	27.9	71.4	100.0	61.7	39.4	22.7	24.2	13.3
	4.0	39.8	83.2	100.0	61.3	58.3	29.5	36.0	20.4
	6.0	34.9	77.9	100.0	57.7	39.9	26.3	31.2	18.1
5.0	0.1	100.0	33.3	11.2	0	0	0	0	0
	0.5	100.0	59.5	7.0	1.2	0	0	0	0
	1.0	100.0	76.6	16.5	1.5	0.7	0.3	0.2	0.5
	2.0	100.0	99.7	39.8	7.0	1.4	0.5	0.3	0.6
	4.0	63.1	100.0	69.7	18.1	8.3	1.7	1.3	1.0
	6.0	52.3	100.0	84.9	28.3	15.1	4.6	3.2	1.9
	10.0	47.2	100.0	97.1	41.0	21.9	6.9	6.3	2.5
10	0.1	100.0	30.8	2.6	0	0	0	0	0
	0.5	100.0	38.3	3.0	0.3	0.2	0.2	0.1	0.4
	1.0	100.0	52.4	4.8	0.4	0.3	0.2	0.1	0.3
	2.0	100.0	57.6	7.4	0.8	0.3	0.2	0.1	0.3
	4.0	100.0	76.3	14.0	1.4	0.4	0.3	0.2	0.3
	6.0	100.0	95.6	32.0	4.1	1.1	0.5	0.4	0.4
	7.5	92.5	100.0	38.4	5.5	1.6	0.4	0.2	0.5
20	0.1	100.0	3.1	3.1	0	0	0	0	0
	0.5	100.0	48.4	4.4	0.4	0.4	0.4	0.3	0.6
	1.0	100.0	47.1	4.0	0.4	0.4	0.3	0.2	0.5
	2.0	100.0	47.5	4.1	0.4	0.4	0.3	0.2	0.4
	4.0	100.0	48.3	4.1	0.4	0.4	0.3	0.1	0.4
30	0.1	100.0	20.0	1.7	0	0	0	0	0
	0.5	100.0	45.7	3.9	0.6	0.5	0.5	0.6	0.8
	1.0	100.0	46.9	3.9	0.5	0.5	0.4	0.4	0.6
	2.0	100.0	47.0	3.8	0.5	0.5	0.4	0.3	0.6
	4.0	100.0	47.2	3.8	0.4	0.5	0.4	0.3	0.5

[a]Abundances were obtained with spectra from 28 repetitive and averaged scans.

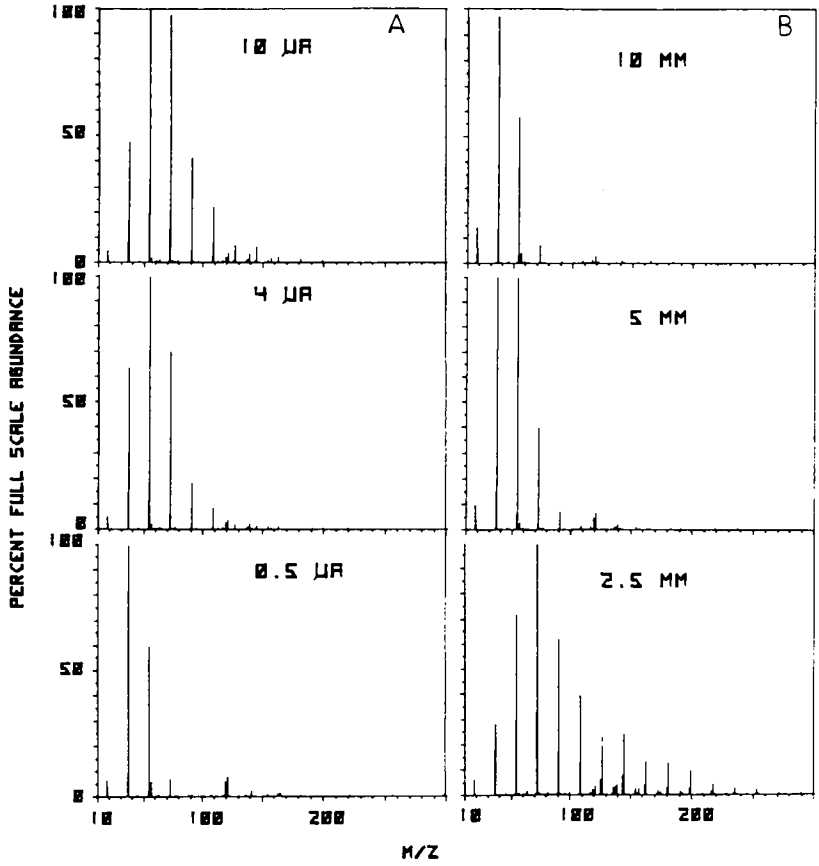

Figure 4 Mass spectra for reactant ions in ambient air from a corona discharge (A) at different currents for a 5 mm gap and (B) at different gap sizes for a 2 μA discharge current. Base peak intensities ($\times 1\,000\,000$) were: (A) 10 μA, 1.84; 4 μA, 2.17; 0.5 μA, 0.008; and (B) 10 mm, 1.63; 5 mm, 1.92; and 2.5 mm, 0.46. All other MS and source conditions were unchanged.

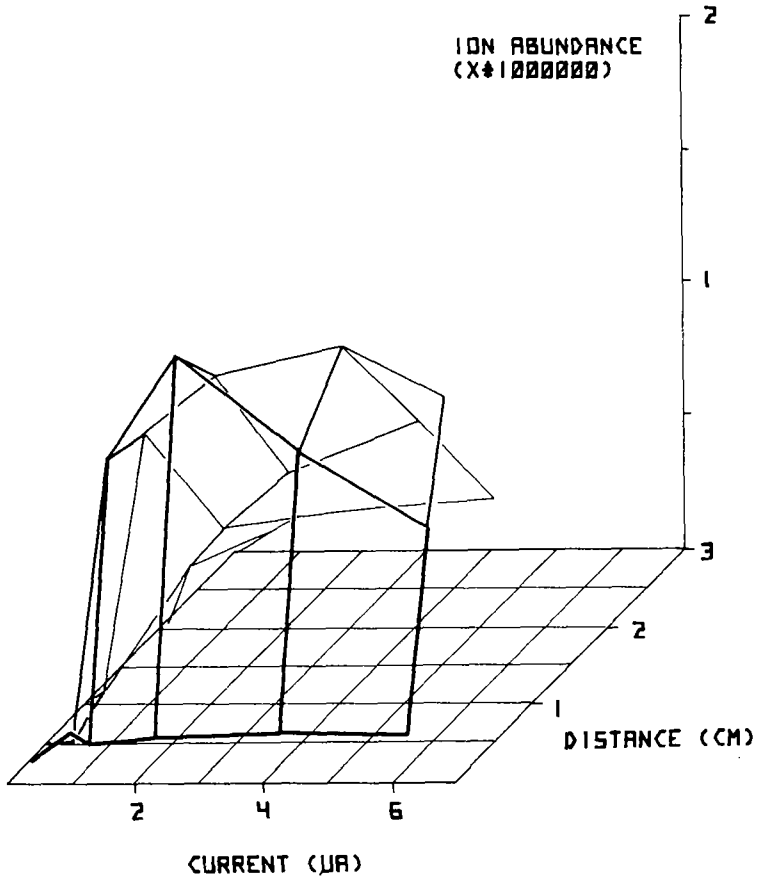

Figure 5 Ion abundance for reactant ion $(H_2O)_2H^+$ (37 amu) in ambient air in corona discharge API-MS. Abundance values were taken from spectra averaged with 28 scans. Comparable plots were also found with other reactant ions although absolute abundances and shapes of envelopes differed slightly. The abundance profile for this ion can be compared directly to the CD operating region in Figure 2.

API-MS determination of analyte in ambient air

In API rate theory for collisional ionizations,[12] the number density of product ions, n_p, is related to total number of available reactant ions, n_r^0, and number density of neutral analyte, N_p, as in Eq. 1:

$$n_p = n_r^0 * k_r * N_p(\alpha * n_{op} - k_r * N_p)^{-1} \quad (1)$$

where the terms are k_r, ionization rate constant for conversion of analyte to product ion; α, recombination coefficient, and n_{op} opposing ion density. This theory was originally developed for electrically non-heated ions in low fields but may also be valid for a CD source with present parameters. Response curves for analyte in air should have a linear region (slope $n_r k_r/\alpha n_{op}$ with increasing N_p until available reactant ions are consumed whereupon the curve becomes level at n_r^0. Thus, if n_r^0 is increased, the upper limit for N_p (linear range) and the product ion intensity (limits of detection) should be improved. However, since n_p is directly proportional to n_r^0, variation in n_r^0 should also propagate through n_p and the reproducibility of n_p should be no better than that for n_r^0. Finally, in low electric field API sources, relative abundances for individual analyte ions in a mixture are related to competitive ionizations through differences in k_r or in proton affinities.

In Figure 6, response curves of n_p versus N_p are shown for three analytes where n_p increased linearly as n_r decreased. Consistent with the available rate theory, larger n_r^0 yielded larger n_p intensities and n_p was fixed or limited by available reactant ion density, n_r^0. However, linear ranges seen for two discharge currents were not noticeably affected as anticipated from different n_r^0 values. Generally, the response curves matched Eq. 1 and suggested that API reactions in the CD conform to low field theory. This was anticipated from E/N calculations that were nearly 10-fold smaller than necessary to accelerate ions at ambient pressures. As seen in curves for reactant ions in Figure 6, decreases in particular reactant ions ($n=2,3$) showed no appreciable discrimination based on differences in proton affinities. No analyte used here caused selective loss of only one reactant ion found in air.

In Figure 7, N_p for DMMP was fixed at a low concentration so reactant ions were not completely depleted. As N_p for EtOAc was

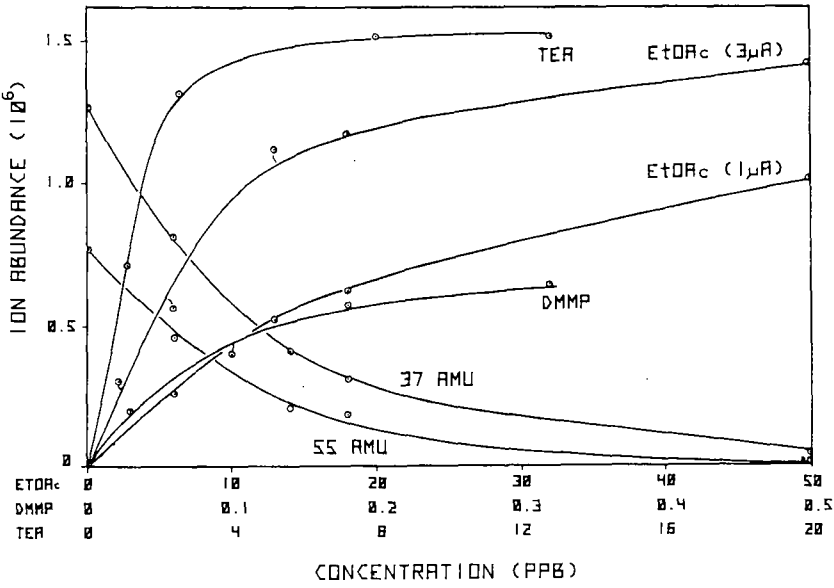

Figure 6 Response curves from a corona discharge ion source in API-MS monitoring of analytes in ambient air. Curves are plots of product ion (MH^+) intensity versus analyte (M) concentrations in air for three analytes: ethylacetate (EtOAc), triethylamine (TEA) and dimethylmethylphosphonate (DMMP). Response curves at two currents of 1 and 3 μA are shown for EtOAc and corresponding reactant ion currents for the two predominant reactant ions (37 and 55 amu) are shown for the EtOAc response at 3 μA. Concentration scales corresponding to depletion of reactant ions differed for each compound and are shown individually at the bottom of the curves.

increased, reactant ions with low proton affinities were consumed preferentially over $(DMMP)H^+$ with higher proton affinity. Parallel decreases in ion intensities for 37 and 55 amu supported earlier findings that product ion formation caused no differences in depletion rates as a function of n in the hydrated cluster ions. However, this study also demonstrated that selective depletion of available proton sources can occur if proton affinities of such sources are sufficiently different such as $(H_2O)_2H^+$ versus $(DMMP)H^+$. This was consistent with prior competitive ionization studies with binary mixtures at atmospheric pressure in ion mobility spectrometry.[17] The presence of analytes with large proton affinities diminish relatively small

distinctions as shown in competitive ion formation with TEA in Figure 7B. Increased concentrations of TEA caused concomitant loss of intensity in both reactant ions and $(DMMP)H^+$ which was a competitor for available charge. Clearly, the unexpected presence of components with large proton affinities in air may have severe analytical consequences for atmospheric monitoring using CD-based API-MS or MS/MS despite excellent MS capabilities for mass analysis. In this regard, a CD source has no inherent advantage over radioactive sources in API-MS or other API-based instruments.

Source parameters and product ions

Effects from current and gas flows on the product ion for EtOAc are shown in Figure 8 as continuous measurements of abundance in SIM plots. Throughout a plot, current was reduced at regular time intervals. When the curtain gas flow was 95 mL/min, peak-to-peak variation in signal abundance exceeded 40% but generally improved with lower currents. However, when the curtain gas was increased to 230 mL/min, instability in ion abundances was diminished and dependence on discharge current was less than with low curtain gas flow. When this flow was set to 400 mL/min, fluctuations were roughly 5% peak-to-peak and a striking 100% change in absolute abundance occurred for MH^+ compared to 95 mL/min. Under conditions of curtain gas flow of 95 to 230 mL/min (20 to 40 cm/s) and air flow of 20 to 100 L/min (100 to 500 cm/s), flows were laminar (Reynolds number < 1200) and confluence occurred in the reaction zone of the CD. Since the linear velocities for ions were 1000- to 10 000-fold larger than those for gas molecules, arguments for differences from ion clustering or declustering through collisions with curtain or sample gas seemed unreasonable. Rather, the effects seen here may be due originally to ion formation or the gas composition in the gap. For example, at curtain gas flows of 95 mL/min, relative abundances for reactant ions were inverted so ion intensities increased $37 < 55 < 73$ amu. However, total ion abundance with a curtain gas of 400 mL/min was only 67% of maximum total ion abundance for a 5 mm gap. Although not tested here, the anticipated control of ion-molecule reactions using contact time may be better approached instead through control of gas composition in the reaction zone. The instability in the MH^+ signal clearly reflected some fluctuation in

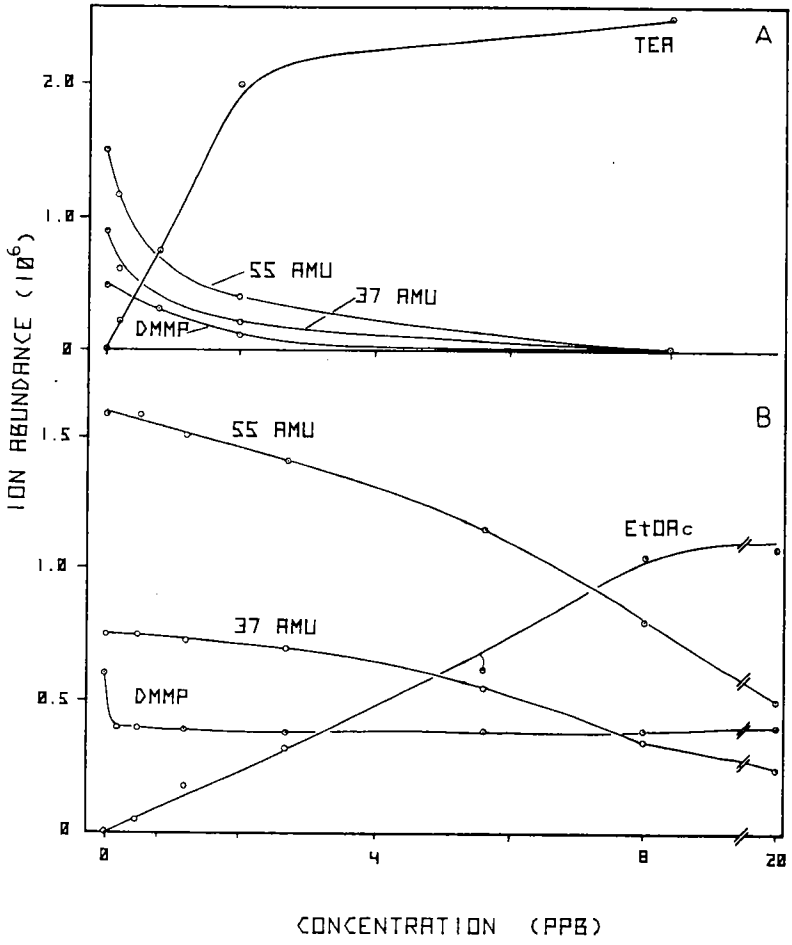

Figure 7 Response curves in API-MS for binary mixtures of analytes in air. In these plots, DMMP was fixed at roughly 0.2 ppb while a second analyte (triethylamine in Frame A and ethylacetate in Frame B) was metered into the CD source. The concentration of the second component is shown on the x-axis and ion intensities for all product ions including two reactant ions are shown.

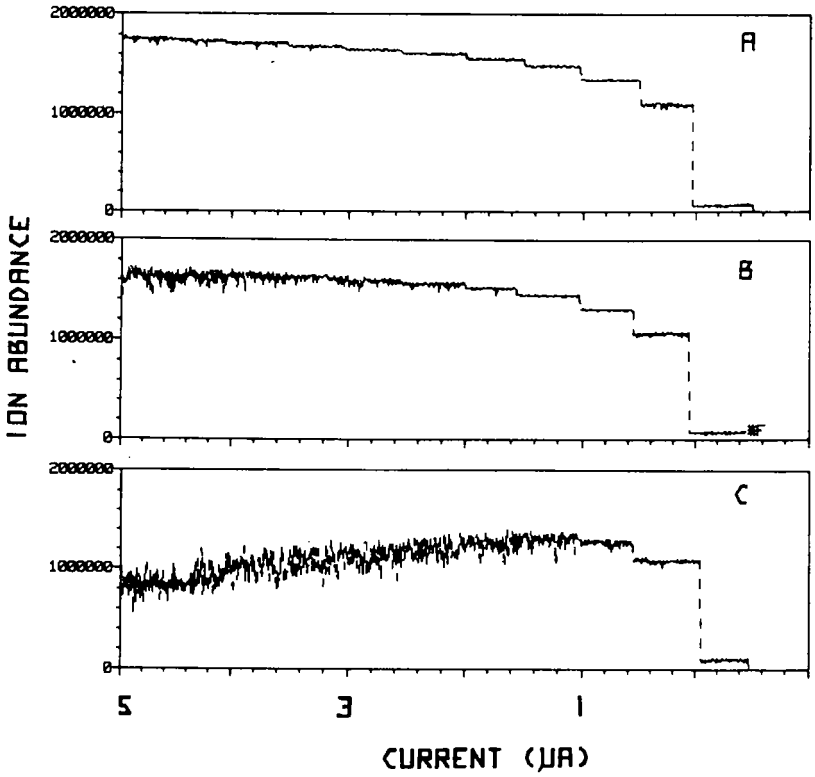

Figure 8 Influence of discharge current strength and curtain gas flow rate on product ion intensities. Ethylacetate at roughly 40 ppb was metered continuously into the source while current was reduced in steps from 5 μA to 1 μA using 0.5 μA intervals. From 1 μA to 0.4 μA the steps were 0.2 μA. The gap size was 5 mm. Curtain gas flows were (A) 300, (B) 200, and (C) 95 mL/min. The flow of sample gas (ambient air) into the CD source was 25 L/min.

the CD discharge region and this may be due primarily to fluctuation in mixing of sample and curtain gases in the discharge gap. Similar results of sensitivity and stability were seen with DMMP and TEA.

In addition to stability and sensitivity in API-MS measurements, the curtain/sample gas flow ratio introduced spectral complications from high mass reactant ions. In Figure 9, this complication is illustrated in mass spectra for DMMP where reactant ions between

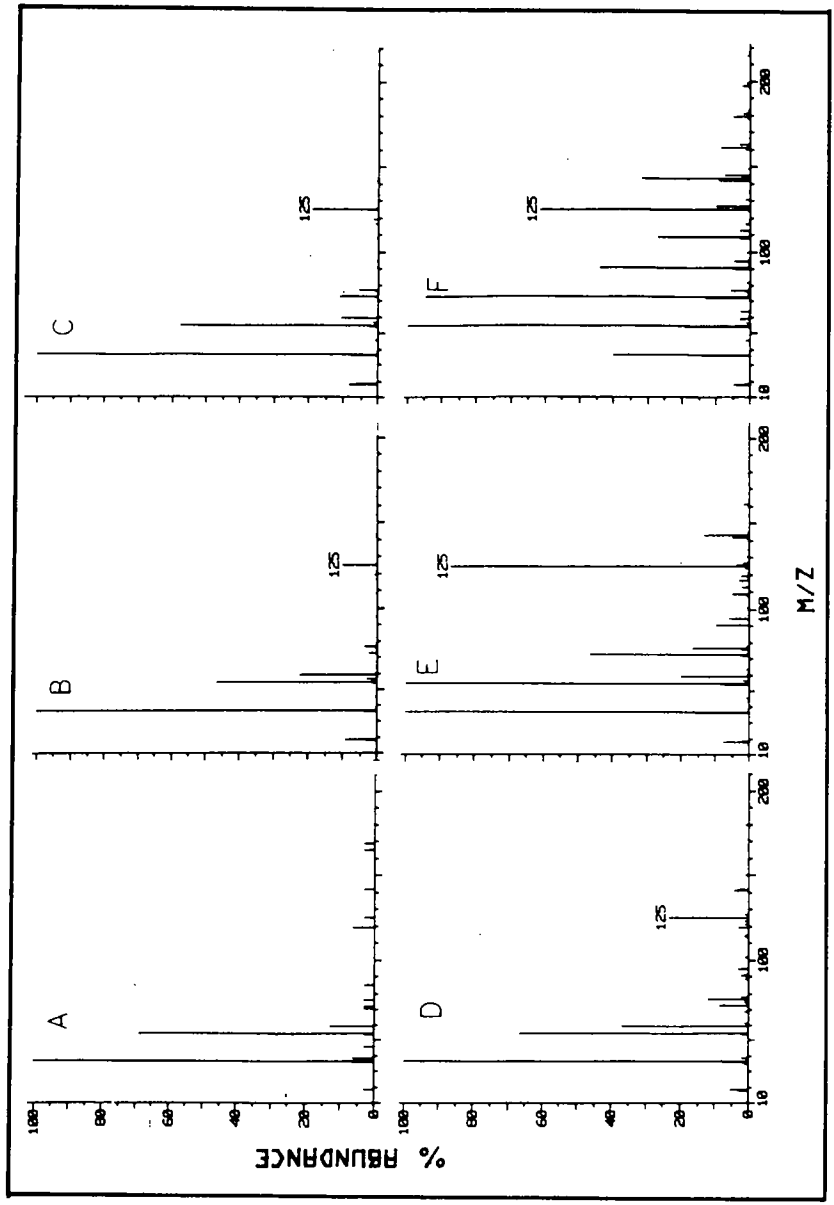

Figure 9 Effect of discharge current and curtain gas flow on the mass spectrum of DMMP in ambient air with a 5 mm gap size. The curtain gas flow was 400 mL/min (A, B, C) and 95 mL/min (D, E, F) and currents were 2 μA (A, D), 4 μA (B, E) and 6 μA (C, F). Absolute intensities for total ion abundances were : (A) 1143, (B) 87 755, (C) 1 935 623, (D) 15 002, (E) 99 400 and (F) 4 227 144.

91 and 163 bracketed the product ion, $(DMMP)H^+$ at 125 amu, despite overall improved intensities. While this interference should not be especially troublesome in API-MS where product ions experience little or no fragmentation, multi-component analysis may become complicated by such species. Otherwise, operation with the source at 10–30 mm gaps and 1–6 μA current will result in reduced complications along with reduced ion intensities. While the influence of higher-hydrated ions has been eliminated in past API-MS analysis through the removal of water molecules attached to ions between the pinhole and a declustering lens,[18] such declustering was not evident here. Changes in the declustering lens voltage yielded near-Gaussian curves for ion abundance versus lens voltage but relative abundances from declustering or other processes were unchanged. Thus, declustering which is observed in other API-MS may be unreliable when a curtain gas is used and ion distributions injected into the MS will be established principally by the dry nitrogen curtain gas. Of course, this conclusion came from only a single investigation of this effect and further examination is warranted.

Since product ions are directly proportional to n_r^0, one last parameter, the role of point-to-plane alignment, was evaluated using only reactant ions. The shape of a corona discharge has been described in Eq. 2 where the terms are y, axial displacement; d, gap size; $j(y)$, current density at y; and j, current density for the on-axis location.

$$j(y) = j\cos^5\theta, \text{ where } \theta \text{ is} \tag{2}$$

$$\theta = \arctan(y/d). \tag{3}$$

Axial displacement of the needle off center at gap sizes of 5 and 10 mm showed current intensities that agreed with Eq. 2 reasonably well until the displacement exceeded 3 mm. However, during this slight displacement, total ion abundances, n_r^0, decreased nearly 40% at 5 mm and $<5\%$ at 10 mm. Total abundances fell below 10% of maximum intensity at a displacement of 3.2 mm for a 5 mm gap and 5.8 mm for a 10 mm gap. Distortion of experimental currents compared to Eqs. 2 and 3 was believed due to the conical rather than flat shape of the discharge plane. Once again, operation of the CD at large gap sizes will lead to a source that is insensitive to source parameters but also to one with poor ion intensities.

CONCLUSIONS

Corona discharge can be used as an ion source for ambient air monitoring in API-MS with maximum precision of better than 10% when source parameters are correctly established; the reputation of CD as an unstable ion source was not supported by these findings. However, source parameters that correspond to high ion intensities also are those which are highly susceptible to slight variations in electrical, physical and flow variables. Product ion formation in API-MS with a CD ion source is governed by molecular properties rather than by user-controlled parameters although reactions may be influenced partly by the existence of a dry nitrogen curtain gas near the reaction zone. No design improvements were clearly evident from findings here although miniature sources with small gap sizes may be prone to instability from size alone. Otherwise, CD use in other atmospheric monitors should be possible, but, should not have inherent advantages based on adjustment of ion-molecule reaction times.

Acknowledgement

Financial support to GAE through the Army Research Office is gratefully acknowledged.

References

1. E. C. Horning, M. G. Horning, D. I. Carroll, I. Dzidic and R. N. Stillwell, *Anal. Chem.* **45**, 936 (1973).
2. D. I. Carroll, I. Dzidic, R. N. Stillwell, M. G. Horning and E. C. Horning, *Anal. Chem.* **46**, 706 (1974).
3. M. M. Shahin, *J. Chem. Phys.* **43**, 1798 (1965).
4. M. M. Shahin, *J. Chem. Phys.* **45**, 2600 (1966).
5. M. M. Shahin, *J. Chem. Phys.* **47**, 4392 (1967).
6. A. Good, D. A. Durden and P. Kebarle, *J. Chem. Phys.* **52**, 212 (1970).
7. I. Dzidic, D. I. Carroll, R. N. Stillwell and E. C. Horning, *Anal. Chem.* **48**, 1763 (1976).
8. G. W. Trichel, *Physical Review* **53**, 214 (1938).
9. M. Goldman and A. Goldman, In: *Gaseous Electronics*, M. N. Hirsch and H. J. Oskam, eds., Academic Press, NY, pp. 234–240 (1978).
10. D. T. Williams, H. V. Denley and D. A. Lane, *Amer. Ind. Hyg. Assoc. J.* **41**, 647 (1980).

11. D. T. Williams, H. V. Denley and D. A. Lane, *Amer. Ind. Hyg. Assoc. J.* **43,** 190 (1982).
12. G. E. Spangler and M. J. Cohen, In: *Plasma Chromatography*, T. W. Carr, ed., Plenum Press, NY, pp. 19–24 (1984).
13. V. J. Vandiver, "Gas phase reaction rate constants for atmospheric pressure ionization in ion mobility spectrometry", Ph.D. Dissertation, New Mexico State University, Las Cruces, NM, May 1987.
14. C. S. Leasure, M. F. Fleischer, G. K. Anderson and G. A. Eiceman, *Anal. Chem.* **58,** 2331 (1986).
15. S. J. Chapman, *Atmos. Sci.* **34,** 1801 (1977).
16. H. E. Revercomb and E. A. Mason, *Anal. Chem.* **47,** 970 (1975).
17. V. J. Vandiver, C. S. Leasure and G. A. Eiceman, *Int. J. Mass. Spectrom. Ion Phys.* **66,** 223 (1985).
18. H. Kambara and I. Kanomata, *Int. J. Mass Spectrom. Ion Phys.* **25,** 129 (1977).